Int J Adv Manuf Technol (2015) 76:1905–1912
DOI 10.1007/s00170-014-6420-4

ORIGINAL ARTICLE

Mechanics of hot pressed aluminum composites

Ahmed Nassef · Medhat El-Hadek

Received: 1 June 2014 / Accepted: 17 September 2014 / Published online: 30 September 2014

Abstract Aluminum powder with an average particle size of 10 μm was mechanically mixed thoroughly with 5 wt% fine Al_2O_3 powder with an average particle size of 3.7 μm reinforcement. Iron particles with an average particle size of 0.5 nm and copper particle size of 10 μm were added to the base matrix Al–5Al_2O_3. The composite material was produced by a single action hot compaction of the powders. Aluminum–alumina composites containing iron, copper, and iron with copper were produced through mixing the atomized matrix alloy powder with 5 wt% of Al_2O_3 particles, then cold pressed for 5 min, degaussed, and hot pressed. The hot pressing technique was performed up to 500 °C at 318.34 MPa for 5 min dwell time. The Al–5Al_2O_3 composites were examined for hardness, compression flow properties, and wear analysis.

Keywords Metal matrix composites · Hot pressing process · Dry sliding wear

1 Introduction

Powder metallurgy processing has a large domain of applications because of their low cost, flexibility complex alloy shapes, wide range of reinforcement elements, and in metastable structures of applications [1, 2]. Homogeneous distribution of the reinforcement in the matrix could be easily achieved using powder metallurgy technique without the severe matrix reinforcement reaction. This is often a disadvantage in traditional techniques, such as squeeze infiltration or stir casting of the alloying elements in the molten matrix composites.

Metal matrix composites (MMCs) incubating alloying elements such as ceramic particulates, improves the mechanical, and wear properties as a result of restricting the deformation of material during mechanical processing [3, 4]. Alumina (Al_2O_3) is one of the most economical and broadly used materials of the ceramics family. Due to the light weight of the Al–Al_2O_3 metal matrix composites, they are utilized in the applications of aerospace and automobile industries [5]. Furthermore, Al–Al_2O_3 metal matrix composites possess many other desirable properties relative to its weight such as high modulus of elasticity, disdainful hardness values, superior compression strength, and wear resistance [5]. Aluminum enforced with ceramic particles as Al_2O_3, SiC, TiC, and TiB_2 is widely used for structural parts as they possess high toughness and superior wear resistance [6]. The melting temperature of Al_2O_3 is 2045 °C, whereas the melting temperature of aluminum is 660 °C with the addition of processing high electrical and thermal conductivities [7]. Lately, aluminum metal matrix composites were utilized in the manufacturing of traditional engine parts as diesel engine pistons, high performance propelling shafts, intake manifolds, and disk brakes especially for light weight hybrid vehicles [8]. Aluminum metal parts provide many benefits to products such as improved corrosion resistance, increased solderability, reduced friction, enhanced paint adhesion, and increased magnetism. Recent investigation shows that the use of submicron $A1_2O_3$ in aluminum metal matrix composites enhances the machinability and decreases the parts cost and increase engineering usage [9, 10].

A. Nassef · M. El-Hadek (✉)
Department of Production & Mechanical Design, Faculty of Engineering, Port-Said University, Port-Said, Egypt
e-mail: melhadek@gmail.com

M. El-Hadek
e-mail: melhadek@eng.psu.edu.eg

A. Nassef
e-mail: nassef12@yahoo.com

Since the mechanical properties restrict the materials applications, it is essential to produce composites, which are adequately homogeneously shaped, with low porosity, and consistent microstructure [11, 12]. However, it is difficult to fabricate metal composites with large amounts of non-metallic ceramic particles, due to the low green density and strength. These metallic and non-metallic composites have inadequate strength to support secondary processing especially sintering and workability. In addition, at high volume fractions of alloying elements, the inclusions support a part of applied pressure elastically by generating a long range network, resulting in the reduction of the pressure on the compact plastic phase [13, 14]. Silicon particles embedded in the aluminum matrix with different particle sizes and volume fractions were studied by Kiser et al. [15]. Wang et al. [16] studied the effect of reducing the allying element particle size from the micro level to nano level on the microstructure, where it was found that the rigidity and the strength of the aluminum matrix increased significantly [16].

The purpose of the present study was to manufacture four different MMCs using hot pressed powder alloying process, namely Al–5Al_2O_3, with no additions, Al–5Al_2O_3 + 0.5 Fe, Al–5Al_2O_3 + 1 Cu, and Al–5Al_2O_3 + 0.5 Fe + 1.0 Cu use hot pressing. Study the iron and copper alloying the effect of the hardness, mechanical flow behavior, and wear properties of the Al–Al_2O_3 metal matrix composites.

2 Materials preparation and processing

2.1 Preparation of MMC

Commercially pure aluminum powder with an average particle size of 10 μm and 99.99 % purity was mechanically mixed thoroughly with 5 wt% very fine Al_2O_3 powder with average particle size of 3.7 μm and a density of 2.9 g/cm^3 reinforcement. The particles used in this analysis where iron with an average particle size of approximately 10 μm and copper with an average particle size of approximately 10 μm and 99.5 % purity made by Aldrich-Germany. The weights of powders were designed to produce specimens of the compositions namely as pure Al–5Al_2O_3, Al–5Al_2O_3 + 0.5 Fe, Al–5Al_2O_3 + 1 Cu, and Al–5Al_2O_3 + 0.5 Fe + 1.0 Cu. The particles were mechanically mixed using SPEX 8000 M MIXER/MILL. The mixture was compacted (cold pressed) at laboratory temperature to get 30 mm diameter and 50 mm height of the green compact using an hydraulic press of the Dorst type of 40 t in capacity. In order to take the initial pressed density into consideration, the compact sinterability was computed in terms of densification parameter (ΔD) as a proportional function of (sintered–green)/(theoretical–green) densities. The theoretical density (ρ_t) was estimated as:

$$\rho_t = \frac{\rho_1 + \rho_2}{\rho_1 . w_2 + \rho_2 . w_1} \quad (1)$$

where ρ_i and w_i are the elements of theoretical density and weight fraction, respectively.

2.2 Hot pressing method

The setup assembly for hot pressing was based upon heating to 500 °C for the duration of 30 min prior to sintering. The heated compacts were then hot pressed for getting proper densification, and then the green compact was sintered to decrease the porosity. The compacting pressure increases gradually to reach up to 314.38 MPa with constant crosshead speed of 2 mm/min. Afterward, a solution treatment was applied for hot pressed specimens at 550°C for 2 h, followed by quenching in water. All hot pressed MMCs were heat treated at about 550°C to allow the copper and aluminum atom to diffuse randomly into a uniform solid solution. Hot compaction was performed in a single-acting piston cylinder arrangement, as shown in Fig. 1. The die bore was smeared with graphite powder reduce die-wall friction, and desired weights of mixed composites are used for each compact. A hydraulic testing machine of 40 t capacity was used to perform the compaction of the alloy powder with constant cross head velocity of 0.002 m/min. The height of green compact was measured directly before and after ejecting from the die. The final height is also calculated from the load-displacement curve. After unloading, the elastic recovery of the compacts is neglected [17]. A compacting pressure ranging from 227 to 909 MPa was calculated by assuming that the cross section of the compact is equal to that of the die. The temperature of the die was measured using NiCr–Ni thermocouple inserted into the die and maintained at the die cavity. The temperature was preserved at the required level with a tolerance of ±5 °C. Different mold temperatures are tested up to 500 °C at the constant pressure of 314.38 MPa and constant crosshead speed of 2 mm/min. The cylindrical disc specimen has an outer diameter of 45 mm.

The setup was heated to the predefined temperature level and maintained constant for 30 min for homogenous distribution within the powder alloy. The forming pressure was lowered for all tested hot components. After the compact operation, the samples were covered with aluminum foil and embedded in a graphite powder to protect its surface from the oxygen and nitrogen from the atmosphere during the sintering process. The specimens were sintered at a steady heating rate of 20 °C/min up to 550 °C for 1 h. The temperature was maintained at that level with a tolerance of ±5°C.

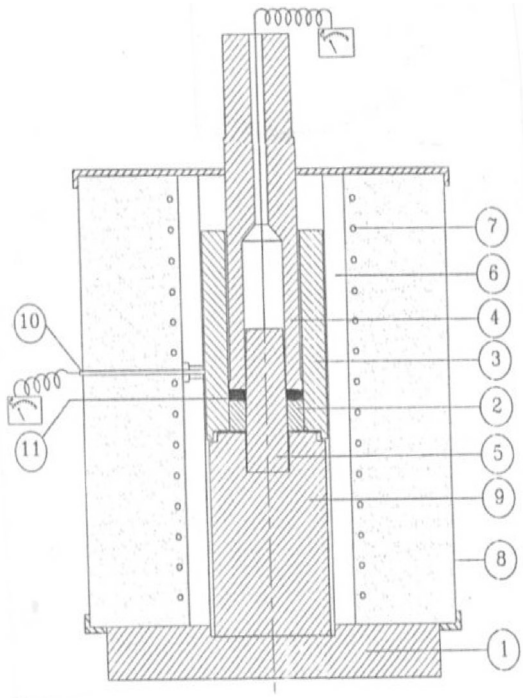

Fig. 1 Die set up of the hot pressing technique

2.3 SEM measurements

Scanning electron microscopy (SEM) optical investigation was conducted on the compositions namely as pure Al–5Al_2O_3, Al–5Al_2O_3 + 0.5 Fe, Al–5Al_2O_3 + 1 Cu, and Al–5Al_2O_3 + 0.5 Fe + 1.0 Cu after the preparation process. Microscopic examination was performed using a Jeol 5400 SEM unit with a Link EDS detector attachment to observe the particle morphology, particle size, particle shape, and agglomeration of particles. Figure 2 shows the microstructure of the hot pressed four Al with various powder element additions.

2.4 Mechanical uniaxial compression

Compression tests were conducted with an Instron 8562 universal mechanical tester under quasi static loading

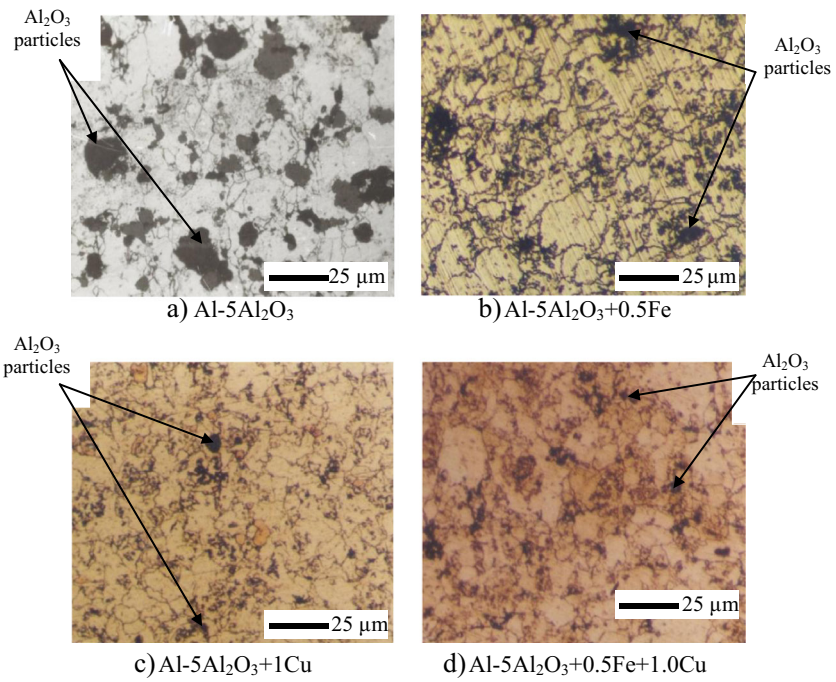

Fig. 2 The microstructure of hot pressed Al–5Al_2O_3 composites with various powder element additions, *dark arrows* refer to Al_2O_3 particles. **a** Al–5Al2O3, **b** Al–5Al2O3 + 0.5 Fe, **c** Al–5Al2O3 + 1 Cu, and **d** Al–5Al2O3 + 0.5 Fe + 1.0 Cu

and strain rate of $8\times10^{-5}\pm5$ %/s at laboratory temperature. Cylindrical specimens were prepared with a diameter of 3 mm and height of 5.5 mm from cast rods. The samples were deformed until failure. To ensure consistency and homogeneity, three identical samples were prepared for each test case and exposed to the same loading conditions. The mean test value of all the three samples was reported in the results. The stress–strain responses of the four compositions namely as pure Al–$5Al_2O_3$, Al–$5Al_2O_3$ + 0.5 Fe, Al–$5Al_2O_3$ + 1 Cu, and Al–$5Al_2O_3$ + 0.5 Fe + 1.0 Cu were measured from uniaxial compression testing performed accordingly to ASTM standard E-9 for metals. The crosshead speed was 1 mm/min.

2.5 Wear testing

Dry sliding wear tests were conducted for the four types Al–$5Al_2O_3$ composites against stainless steel using pin-on-disc apparatus. The asperities of the harder material surface of the stainless steel using a pin-on-disc apparatus were a ploughing action on the surface of the Al–$5Al_2O_3$ composites. The wear resistance of the four compositions namely as pure Al–$5Al_2O_3$, Al–$5Al_2O_3$ + 0.5 Fe, Al–$5Al_2O_3$ + 1 Cu, and Al–$5Al_2O_3$ + 0.5 Fe + 1.0 Cu was investigated using a pin-on-disk abrasive wear tester [18, 19]. The wear specimens were 8 mm in diameter and 12 mm in length. Surface preparation was conducted before the wear test, where each specimen was ground with 1-μm alumina suspension. Wear tests were conducted under dry sliding conditions, applied loads of 10 N, and a constant sliding speed of 1.8 m/s. The time of wear was 10 min, and the track diameter was 120 mm for all samples. Wear loses were obtained by calculating the weight loss of the specimens before and after the testing using an electronic balance with sensitivity of 0.1 g. The samples were cleaned in an acetone bath and dried using hot air before the tests to remove organic substances. For each specimen, the wear tests were conducted under constant wear pressure of 3 MPa, sliding distance ranging from 450 to 1800 m, and laboratory temperature conditions. The resulting specimen mass and height were recorded to calculate the weight loss, Δw and wear rate, $W(t)$ in terms of volume loss, and the specific wear rate as W_s [18]:

$$W(t)=\frac{\Delta w}{\rho . t}, Ws=\frac{W(t)}{V_s . F_n} \tag{2}$$

where V_s is sliding velocity in m/s and F_n is the input weight or normal load in N in kg/m/s at constant temperature.

3 Discussion

3.1 Optical investigations

The microstructure investigation on the Al–$5Al_2O_3$ based composites was conducted to observe the particle morphology, particle size, particle shape, and agglomeration of particles after the fabrication process. Figure 2a–d shows the microstructures of hot pressed Al–$5Al_2O_3$ composites namely as pure Al–$5Al_2O_3$, Al–$5Al_2O_3$ + 0.5 Fe, Al–$5Al_2O_3$ + 1 Cu, and Al–$5Al_2O_3$ + 0.5 Fe + 1.0 Cu after the preparation process. All compositions process clear grain boundaries.

3.2 Density and hardness

Density measurements of hot pressing Al–$5Al_2O_3$ composites with various alloying additions are recorded before and after sintering. A significant density increase was noticed after the sintering process was applied for hot pressed composites. The sintering density of the hot pressed composites was greater than 95 %. Comparing Al–$5Al_2O_3$ composites with the additive elemental powder gave better green and sintered density as presented in Table 1. To insure consistency of the Vickers hardness values across the material surface, a minimum of ten readings were accounted for all the cases and calculated as presented in Table 1.

Table 1 shows that the densification parameter increases linearly with the addition elemental powder Fe or Cu. Vickers hardness calculations were conducted with a 10 kg load. The addition of 1.0 Cu and 0.5 Fe + 1.0 Cu increases the HV of the composite from 65 to 130 kg/mm approximately to the double, while the addition of 0.5 Fe to the composite shows no significant change in the hardness value.

Table 1 Densities, densification, and Vickers hardness measurements of the four Al–$5Al_2O_3$ composites

Composites	Density (g/cm)			Densification parameter	Vickers hardness (kg/mm)
	Theoretical	Green	Sintered		
Al–$5Al_2O_3$	2.691	2.213	2.425	0.4435	65
Al–$5Al_2O_3$ + 0.5 Fe	2.699	2.342	2.554	0.5938	79
Al–$5Al_2O_3$ + 1 Cu	2.710	2.375	2.576	0.6	120
Al–$5Al_2O_3$ + 0.5 Fe + 1.0 Cu	2.7188	2.431	2.662	0.8026	130

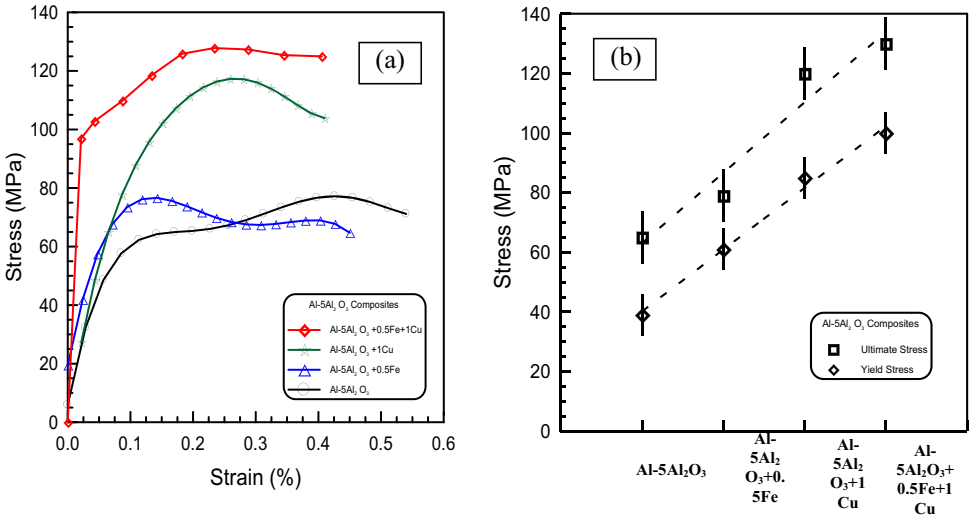

Fig. 3 **a** Compression stress–strain curves and **b** yield and ultimate strengths, for Al–5Al_2O_3 composites with alloying elements

3.3 Compression measurements

The results indicated a measurement variation less than 7 % and crosshead speed of 1 mm/min. Stress–strain behaviors of Al–5Al_2O_3 composites are shown in Fig. 3a with the various powder additives. The addition of Cu or Fe alloying elements to the base composites improved the strength but reduced the ductility of the composite system. The ultimate composite strength of the composites Al–5Al_2O_3 + 1 Cu and Al–5Al_2O_3 + 0.5 Fe + 1.0 Cu was equal to 1.5 times the composite system without additive elements or with the addition of 0.5 Fe to the base matrix Al–5Al_2O_3 as presented in Fig. 3b.

Stress–strain behavior presented in Fig. 3a for the four Al–5Al_2O_3 composites show an improvement in the strength but a reduction in the ductility of the composite system with the addition of Cu or Fe alloying elements to the base composites. Figure 3b shows that the linear yield and ultimate stresses increased with the addition of the alloying elements. The compression flow behavior of the Al–5Al_2O_3 composites was calculated from the mechanical flow parameters [11] and presented in Table 2. The strength coefficient (K) and the strain hardening exponent n for composites with Cu element are higher than that of other composites. The analysis of the results shows that the 0.5 wt% addition of iron to Al–5Al_2O_3 composite has a negative effect on the mechanical flow properties of the aluminum composite matrix. This was explained by the precipitation of intermetallic compound on the grain boundaries of aluminum [20]. The flow properties of the Al–5Al_2O_3 composites show improvement as an alloying elements as illustrated in Table 2, especially for Fe addition. The compression flow stress of Al–5Al_2O_3 composites containing Cu was higher than those of Al–5Al_2O_3 composites without Cu particles. The lowest value was obtained when the iron Fe was added.

Table 2 The mechanical flow properties of composite materials of the four Al–5Al2O3 composites

Composites	Properties		
	K (MPa)	n value	R^2
Al–5Al_2O_3	106	0.331	0.918
Al–5Al_2O_3 + 0.5 Fe	97	0.221	0.984
Al–5Al_2O_3 + 1 Cu	263	0.502	0.901
Al–5Al_2O_3 + 0.5 Fe + 1.0 Cu	172	0.152	0.932

The flow properties of the Al–5Al_2O_3 composites show improvement as alloying elements are added as illustrated in Table 2, especially for Fe addition. The compression flow stress of Al–5Al_2O_3 composites containing Cu was higher than those of Al–5Al_2O_3 composites without Cu particles. The lowest value was obtained when the iron Fe was added.

3.4 Wear analysis

Apparently, Al–5Al_2O_3 composite base matrix exhibits the highest wear rate, whereas Al–5Al_2O_3 composites with Fe + Cu additives have the smallest wear rate. The addition of Fe and Cu elements to Al–5Al_2O_3 composite decreases the wear rate, which performs as an obstacle to the shear deformation as the material is sliding on the counterface. A slight decrease in wear rate for the sliding distance ranging from 450 to 1800 m of Al–5Al_2O_3 composites was found. At this range of sliding distance, the wear rate of Al–5Al_2O_3 composites was equal to double the wear rate for Al–5Al_2O_3 composites with different additive elemental powders. At sliding distance of 450 m, the wear rate of the Al–5Al_2O_3 composites was about 12 times of wear rate for Al–5Al_2O_3 composites with the different additive elemental powders. Figure 4b shows the variation of wear rate with sliding distance for the Al–5Al_2O_3 composites. With the addition of the additive elemental

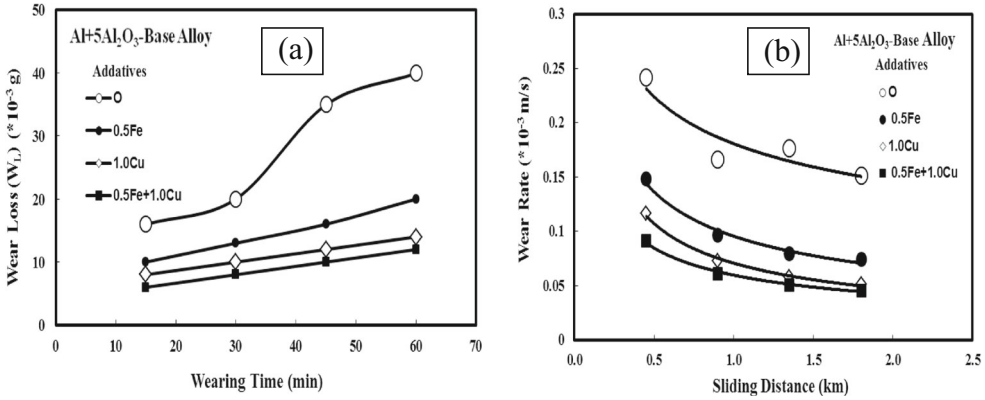

Fig. 4 **a** The variation of wear losses with wearing time, and **b** the variation of wear rate with sliding distance, for Al–5Al_2O_3 composites with alloying elements

powders of 0.5 Fe, 1.0 Cu, or 0.5 Fe + 1.0 Cu, the wear rate decreases respectively. This could be explained due to the increase of the strength with the addition of the additive elemental powders as 0.5 Fe, 1.0 Cu, or 0.5 Fe + 1.0 Cu, respectively.

The wear mechanism of the investigated materials consisted of plastic deformation of the aluminum binder phase and brittle cracking of Al_2O_3 grains [21, 22]. When the binder content increased the wear increased. Materials with higher amount of aluminum in the microstructure exhibit higher wear resistance due to the less bulk hardness. For lower binder content, the brittle cracking of aluminum grains was the dominant reason for wear. It was noticed that the number of grooves on the surface of Al–5Al_2O_3 composite were less than those formed in Al–5Al_2O_3 with added Fe + Cu elements, as presented in Fig. 5, as pointed with the red arrows. This could be explained by the particulate bonding that is higher for the Al–5Al_2O_3 + 0.5 Fe + 1.0 Cu composites and the surface homogeneity was observed by comparing Fig. 5b, c, d. Note that in Fig. 5b for Al–5Al_2O_3 + 0.5 Fe, the Fe particles are shown at point 1, the Al_2O_3 particles are shown at points 2 and 4, the dislocation cavities are shown at point 3, and the grain boundaries are shown at points 5 and 6. A similar observation was recently reported by Balasubramanian et al. [23] as the alumina enhanced the hardness, impact strength, and wear resistance of the Al composites. Additionally, it was evident that with the increase of the alloying elements in the composites, the weight loss decreased in the three alloyed Al–5Al_2O_3 compositions. Al–5Al_2O_3 + 0.5 Fe + 1.0 Cu composite shows less weight loss and better wettability as the adhesion forces

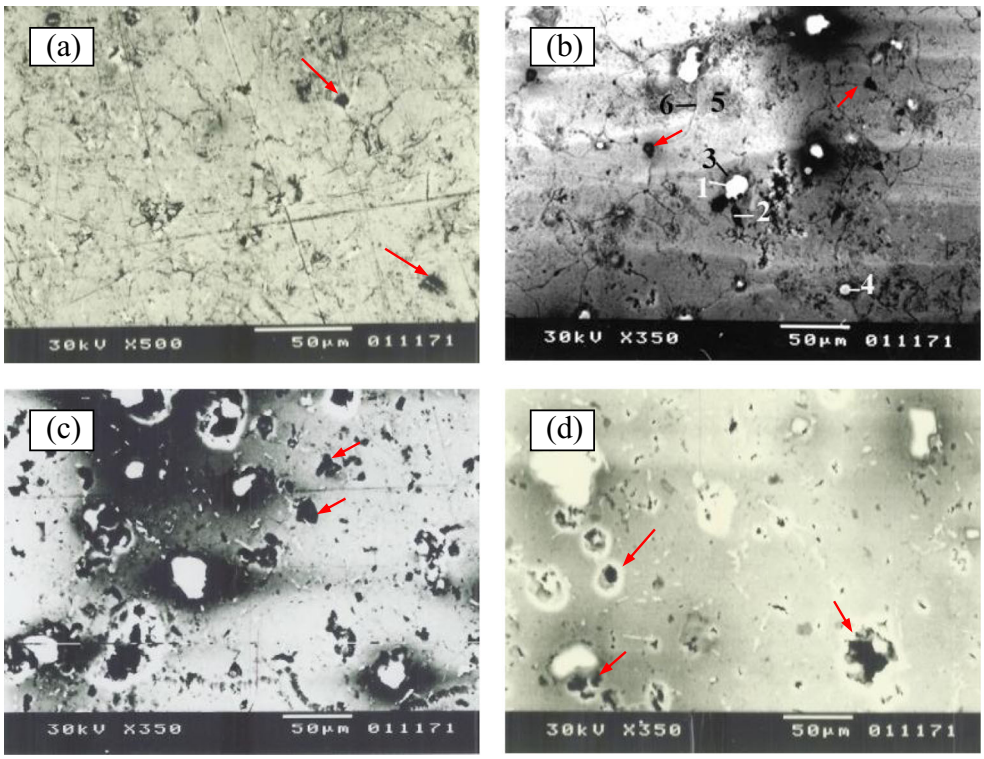

Fig. 5 SEM of the worn surface for **a** pure Al–5Al_2O_3 composite, **b** Al–5Al_2O_3 + 0.5 Fe with a description of the Fe particles at point 1, Al_2O_3 particles at points 2 and 4, and the dislocation cavities at point 3, and grain boundaries at points 5 and 6 also shown with the *red arrows*, **c** Al–5Al_2O_3 + 1 Cu composite, and **d** Al–5Al_2O_3 + 0.5 Fe + 1.0 Cu composite, after wear test

between the particles increases and the presence of the pores between the particles decreases.

Note that in Fig. 5b for Al–5Al_2O_3 + 0.5 Fe, the Fe particles are shown at point 1, the Al_2O_3 particles are shown at points 2 and 4, the dislocation cavities are shown at point 3, and the grain boundaries are shown at points 5 and 6. Additionally, it was evident that with the increase of the alloying elements in the composites, the weight loss decreased in the three alloyed Al–5Al_2O_3 compositions. Al-5Al_2O_3 + 0.5 Fe + 1.0 Cu composite shows less weight loss and better wettability as the adhesion forces between the particles increases and the presence of the pores between the particles decreases.

4 Conclusion

From the mechanical and wear experiments presented on Al–5Al_2O_3 composites, it could be concluded that:

1. The hot pressing technique was suitable to produce dense powder metallurgy parts.
2. For the green Al–5 Al_2O_3 compact powders, the density change was affected by sintering conditions and by the volume fraction with a weight percentage of the alloying element powders.
3. The addition of Fe and Cu to the Al–5Al_2O_3 improves the hardness and reduces the wear losses of the hot pressed alloy.
4. Improvement in the ultimate strength can be obtained by adding the copper or Fe + Cu powders to the alloy matrix.
5. At sliding distance of 450 m, the wear rate was about 12 times of Al–5Al_2O_3 composites with different additive elemental powders, decreasing with the increase of the sliding distance.
6. The method of manufacture has a considerable influence on the properties of the dispersion strengthened aluminum alloys. This work can be considered as one step ahead in the process of rationalization of the role of the percentage of Al2O3 and the other additives in governing the hardness, strength, and wear properties of Al–5Al2O3 metal matrix composites. Improvement in strength and wear properties of Al–5Al2O3 by increasing of the additive percentage (Cu and Fe) has been observed.

References

1. Yan BH, Wang CC, Liu WD, Huang FY (2000) Machining characteristics of Al_2O_3/6061Al composite using rotary EDM with a disk-like electrode. Int J Adv Manuf Technol 16:322–333. doi:10.1007/s001700050164
2. Manna A, Bhattacharayya B (2005) Influence of machining parameters on the machinability of particulate reinforced Al/SiC–MMC. Int J Adv Manuf Technol 25:850–856. doi:10.1007/s00170-003-1917-2
3. Bhushan RK, Kumar S, Das S (2010) Effect of machining parameters on surface roughness and tool wear for 7075 Al alloy SiC composite. Int J Adv Manuf Technol 50:459–469. doi:10.1007/s00170-010-2529-2
4. El-Hadek MA, Kaytbay S (2009) Al_2O_3 particle size effect on reinforced copper alloys: an experimental study. Strain 45:506–515. doi:10.1111/j.1475-1305.2008.00552.x
5. Sameezadeh M, Emamy M, Farhangi H (2011) Effects of particulate reinforcement and heat treatment on the hardness and wear properties of AA 2024-$MoSi_2$ nanocomposites. Mater Des 32:2157–2164. doi:10.1016/j.matdes.2010.11.037
6. Sarajan Z, Soltani M, Khabushan JK (2011) Foaming of Al-Si by TiH_2. Mater Manuf Process 26:1293–1298. doi:10.1080/10426914.2011.551964
7. Şahin Y (2011) Wear behavior of Al-Al2O3 reinforced composites. Adv Mater Res 308:1577–1581. doi:10.4028/www.scientific.net/AMR.308-310.1577
8. Tjong SC, Huo HW (2009) Corrosion protection of in situ Al-based composite by cerium conversion treatment. J Mater Eng Perform 18:88–94. doi:10.1007/s11665-008-9264-y
9. Fallah A, Aghdam MM, Kargarnovin MH (2013) Free vibration analysis of moderately thick functionally graded plates on elastic foundation using the extended Kantorovich method. Arch Appl Mech 83:177–191. doi:10.1007/s00419-012-0645-1
10. El-Hadek MA, Kaytbay S (2013) Characterization of copper carbon composites manufactured using the electroless precipitation process. Mater Manuf Process 28:1003–1008. doi:10.1080/10426914.2012.736662
11. Nassef A, El-Nasser GA, El-Boghdady AA (2033) Mechanical and microstructure characteristics of Al-4Cu/Al2O3 MMCs produced Via PM techniques. J Eng Appl Sci Fac Eng Cairo Univ 50:371–386
12. Seo YH, Kang CG (1999) Effects of hot extrusion through a curved die on the mechanical properties of SiCp/Al composites fabricated by melt-stirring. Compos Sci Technol 59:643–654. doi:10.1016/S0266-3538(98)00123-7
13. Khademian M, Alizde A, Baharvandi H, Majidi H (2013) Comparison of properties and microstructure of A356-B4C nano composites, produced by two methods of casting vortex and semi-solid casting. Bull Pur Appl Sci Phys 32:51–58
14. Li Y, Ramesh KT, Chin ESC (2007) Plastic deformation and failure in A359 aluminum and an A359-SiCp MMC under quasistatic and high-strain-rate tension. J Compos Mater 41:27–40. doi:10.1177/0021998306063351
15. Kiser MT, Zok FW, Wilkinson DS (1996) Plastic flow and fracture of a particulate metal matrix composite. Acta Mater 44:3465–3476. doi:10.1016/1359-6454(96)00028-6
16. Wang F, Zhang K, Zhu J, Ye L (2013) Effect of Mn content on the microstructure and mechanical properties of (Ti, Mn) Al/Al2O3 in situ composites prepared by hot pressing. J Mater Res 28:1574–1581. doi:10.1557/jmr.2013.146
17. German RM (2005) Powder metallurgy & particulate materials processing. Metal powder industries federation, Princeton, NJ, 0-9762057-1-8
18. Yasmin T, Khalid AA, Haque MM (2004) Tribological (wear) properties of aluminum-silicon eutectic base alloy under dry sliding condition. J Mater Process 153:833–838. doi:10.1016/j.jmatprotec.2004.04.147
19. Dutta I, Quiles FN, McNelley TR, Nagarajan R (1998) Optimization of the strength-fracture toughness relation in particulate-reinforced aluminum composites via control of the

matrix microstructure. Metall Mater Trans A 29A:2433–2446. doi:10.1007/s11661-998-0119-9

20. Kaytbay S, El-Hadek MA (2014) Wear resistance and fracture mechanics of WC–Co composites. Int J Mater Res 105:557–565. doi:10.3139/146.111069
21. Kumar GBV, Rao CSP, Selvaraj N (2011) Mechanical and tribological behavior of particulate reinforced aluminum metal matrix composites–a review. J Miner Mater Charact Eng 10:59–91, Paper ID 20824
22. Fleury E, Lee SM, Choi G, Kim WT, Kim DH (2001) Comparison of Al-Cu-Fe quasicrystalline particle reinforced Al composites fabricated by conventional casting and extrusion. J Mater Sci 36:963–970. doi:10.1023/A:1004875824039
23. Balasubramanian KR, Sivapirakasam SP, Anand R (2014) Study on mechanical properties and wear behavior of LM6 aluminum/nano Al2O3 composites. J Appl Mech Mater 592:1352–1356. doi:10.4028/www.scientific.net/AMM.592-594.1352